Chapter 3

Experimental validation of the profile of antitumour entities that enable permanent tumour elimination.

CHAPTER 3: EXPERIMENTAL VALIDATION OF THE PROFILE OF ANTITUMOUR ENTITIES THAT ENABLE PERMANENT TUMOUR ELIMINATION.

3. Outline

According to epidemiological studies, complete spontaneous tumour regression (without therapy), in which the malignancy is completely eradicated, occurs in both human and animals. In order to provide insight into the possibility of therapeutically duplicating such regression processes on tumours clinically, without hazardous side effects, we have formulated in the earlier chapter a novel computational systems biology model for this notable event of tumour extinction by means of negative bias dynamics. Using differential equations that are related to cell dynamics, we have developed an oncological informatics strategy while protecting normal tissue. In the present chapter we investigate three key factors that contribute to tumour lysis: DNA blockage factor, interleukin-2 (IL-2), and cytotoxic T-cells (CD8+ T). Utilizing preclinical experimental studies on malignant tumours, including murine melanoma microarray and histiocytoma immunochemical evaluation, we probed the temporal alteration of these parameters. The temporal changes in the three entities components (DNA replication-blockade factor, Antitumour T-lymphocyte, and IL-2), are characterized respectively by the following temporal profiles: (a) Unimodal Inverted-U function, (b) Bimodal M-function, and (c) Stationary-step function. These three temporal profiles for the three antitumour entities were found to be necessary for the occurrence of permanent tumour regression. These entities offer a tri-phasic cytotoxic milieu that has been timed-orchestrated for eradication of all malignant cells. Additionally, we identified the gene-expression levels related to the three components mentioned above: (i) DNA-damage G2/M checkpoint regulation (CDC2 and CHEK genes);

(ii) Interleukin-2/15 chemokine signalling (IL2RG and IKT3 genes); and (iii) T-lymphocyte signalling (TRGV5 and CD28 genes). The temporal entities of these three components [(i)-(iii)] quantitatively corroborated with the activation profiles that our computational model predicted (Smirnov-Kolmogorov statistical test fulfilled, α = 5%). The ability to eradicate the residual tumour correlates with our observation that the genes CASP7 and GZMB are indicators of Negative bias dynamics. We have provided the dose-time profiles of antitumour agents (DNA alkylator, IL-2, T-cell input) using the negative-biasing approach, so that melanoma tumour may undergo permanent extinction by mimicking the spontaneous tumour regression dynamics.

3.1 Introduction

The quantity of tumour load, the extent of the disease's invasiveness, the rigor of the treatment, and the strength of the patient's immune response are various factors that might affect spontaneous cancer regression (whether it is endogenous or exogenous process). Better treatment plans for cancer patients are being developed using mathematical modelling as a potentially essential tool to combat the cancer regression process. Our previously developed model [20], which uses a system of six differential equations to represent tumour cell kinetics, chemotherapy dynamics, immune system dynamics (NK cell, circulating lymphocyte, and cytotoxic T-cell), chemotherapy dynamics, and immunomodulation/immunotherapy dynamics, has been significantly modified for this study. Our cutting-edge mathematical model is based on biological processes that have been observed in experiments, specifically the lethal effect on the tumour cell caused by the immune cells cytotoxic T-cells (CD8+) and natural killer (NK) cells. The delineation of these lethal interactions are delineated next

It is well established that NK cells target tumour cells and produce cytokines by secreting perforins and granzymes as part of immune responses to malignancies [76, 77].

These immune cells release perforins in the immunological synapse, the perforins are pore-forming cytolytic protein that form porous openings in the tumour cell membrane [23]. Once this occurs, the immune cells release granzyme, which is a proteolytic enzyme that travels through the pore into the cytoplasm of the tumour cell, activating the caspase cascade and thereby inducing programmed cell death or apoptosis in the malignant cell [78]. When NK cells and T-cells come into contact with cancer cells, immunological synapses are formed with tumour cells to deliver lysosome-mediated cytolytic agents (as cathepsins and hydrolases) inside the tumour cells [79]. Moreover, granzymes and perforin are two further examples of cytotoxic chemicals that $CD8^+$ T cells can use to kill tumour cells. Additionally, chemokines as interferons (which cytotoxic $CD8^+$ T-cells secrete) can activate the tumour cells to produce more MHC class I antigens, making the malignant cells to become more attractive targets for cytotoxic $CD8^+$ T-cells [80].

In this study, we want to identify the unitary principles that underlie complete tumour regression (whether endogenous or exogenous) and to quantitatively outline the overall approach of this regression. Thereafter, the validation of the methodology in pre-clinical environment are shown on two malignant systems, melanoma and histiocytoma. To underscore, melanoma cases can undergo fully effective spontaneous regression (PubMed has 585 cases studied in detail [81]), and this melanoma regression occurs appreciably at 10-35% rate [34]. Analysis of 10,098 melanoma regression patients showed that these patients can have incisive clinical correlates [35]. Understanding melanoma regression is critically needed, as it is the type of malignancy whose incidence is accelerating maximally [36]. An important aspect here is that we have showed that a malignant lesion can undergo permanent regression by an optimized synchronization of: 1) antitumour feedback control process, based on optimal dynamic feedback according to tumour load, and 2) normal tissue protection, based on minimization of tissue toxicity, together with 3) ensuring that cancer

stem cells are also eliminated. In contrast to this permanent regression approach, we also show that often conventionally dosed antitumour chemotherapy-immunotherapy intervention (i.e., without dynamic feedback control procedure) fails to eliminate the tumour cells completely, with the result that there is tumour recurrence later.

However, a residual tumour cell population asymptotically exists under the exponentially-decreasing trajectory and this population of residual cells is frequently a factor in tumour recurrence and incurability. It is well-known that three complementary processes can reduce the tumour cell population:

(vii) Decrease of the proliferation of tumour cells: Here, chemical alkylation or chemomodulation of DNA are two methods for reducing cell proliferation that can lead to DNA damage [21, 22],

(viii) Increase of tumour cell lysis: This occurs through the medium of antitumour lymphocytes [23–25],

(ix) Further enhancement of tumour cell lysis: The activation of the antitumour lymphocytes can be boosted by cytokines (for example, immunomodulation by interleukin-2) [26].

It may be underscored that our analysis of the extinction of cancer cells is motivated from the well-known process of spontaneous permanent regression of tumours and its system biology evidence, whereby we have developed an approach of how one can replicate this tumour regression process in a clinical situation. We have provided substantiation of the proposed feedback approach by quantitative analysis of signal transduction pathway, gene expression level of G2/M-phase DNA damage pathway, IL-2 expression and T-cell receptor signaling. Finally, the translational aspects and validated corroboration of our approach is furnished, which enables the formulation of a guided controller-based treatment planning system governing the infusion of chemotherapy,

interleukin, and antitumour T-cell immunotherapy, for complete extinction of the malignant lesion, cancer stem cell elimination and normal tissue protection.

3.2 Materials and methods

3.2.1. Validation of our computational model using experimental biological system

The mathematical model is verified on immunohistochemical experiments and microarray assay of a preclinical model of permanent spontaneous tumour regression in melanoma. Here, numerous tumours appear in pigs, the pigs grow rapidly for the first 1½ months, and then the tumours spontaneously regress completely by 3–4 months in half of the animals, but in the other half, the tumours spread and kill the animals [35]. Schema-1 shows how the malignancy index of the melanoma tumour in a particular pig which displayed complete permanent tumour regression, where the malignant zone of the lesion is represented by yellow and the inflammatory zone in blue. The index decays to negligible values, where the malignancy index indicates the ratio of (actual tumour zone)/(total lesion Zone), the latter zone includes the tumour and inflammatory zone. In our study, six pigs who went into the regression mode, were investigated, tumours had biopsy under anesthesia at three weekly intervals across three months, at five different time points as follows: t_0 = day-of-birth (d) + 8 days after birth (i.e., d + 8), thence $t_1 = d$ + 28 days; $t_2 = d$ + 49; $t_3 = d$+70, and finally $t_4 = d$ + 91 (Schema-2). At each time point 5–6 tumour-masses were biopsied, and subjected to microarray investigation using Ingenuity algorithm.

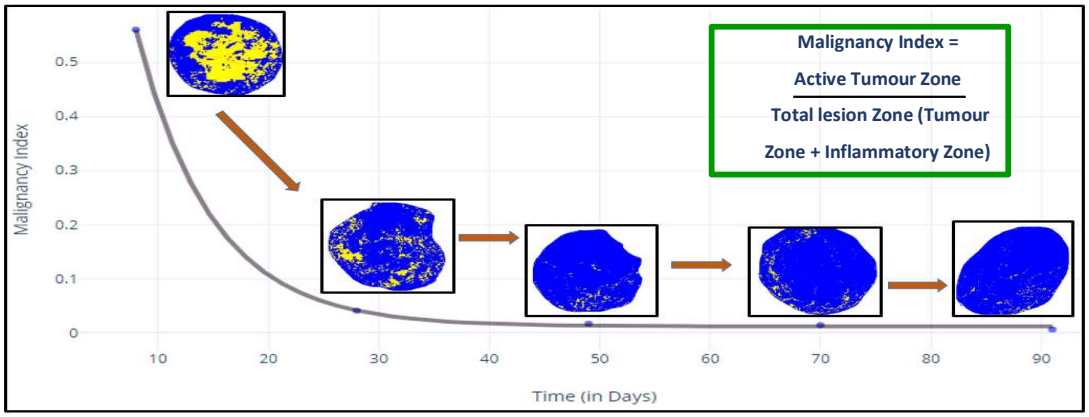

Schema-1. Permanent spontaneous cancer regression of a tumour with time, showing the malignant index attains negligible values.

Time Weeks:	1	4	7	10	13
Time-span (%)	8.8%	30.7%	53.8%	76.9%	100%

Schema-2. Temporal sequence of tumour biopsy analysis across the tumour regression process.

3.2.2 Pre-clinical investigation

Regarding the aforesaid melanoma regression analysis, we accessed the gene expression profiles of E-MEXP-1152 from the ArrayExpress facility (https://www.ebi.ac.uk/arrayexpress/) [37]. The microarray assay was based on Transcription profiling of tumour from the melanoblastoma-bearing Libechov Minipig (MeLiM) model and the Porcine Genome Arrays platform. This involved 5 different tumours of 5 pig siblings, each across 5 time points, from day 8 to day 91 after birth (Submission date: September 10, 2008). Also, the time-dependent gene expression profiling of the spontaneously regressing melanoma tumour biopsies was performed. Further, from the ArrayExpress platform, we analyzed all the raw information CEL-Files

(E-MEXP-1152.raw.1.zip) belonging to this experiment (https://www.ebi.ac.uk/arrayexpress/experiments/E-MEXP-1152/).

3.2.3 Normalization and statistical analysis

We then performed normalization, statistical analysis and the analysis of variance (ANOVA) of the microarray information, using R platform and Bioconductor statistical facility (http://www.bioconductor.org/) [82]. We did the preprocessing step utilizing the GeneChip Robust Multiarray Average (GC-RAM) method to get the gene expression matrix from Affymetrix information. For identification of differentially expressed gene in log_2 scale, we used the Transformation for t-test and one-way ANOVA. Thence, differentially expressed Probe sets were selected on the bases of p value and fold change (FC) value [(FC) > 2 and p value < 0.05]. Moreover, the significant probe sets after ANOVA were used for biological functional analysis and comparison.

3.2.4 Time dependent biological function analysis using pathway study

We then identified the temporal profile of the microarray data for the different Biological Classes category, utilizing the Ingenuity Pathway Analysis procedure (IPA). We also elucidated the expressional changes at each time-point, the functional interpretations, and the biological interaction of the genes, which were also demarcated using IPA. This furnished the temporal pattern of gene-expression levels corresponding to the effector components of Figure 2.5, such as (i) DNA damage (G2/M checkpoint regulation), (ii) Antitumour lymphocyte activation (T-lymphocyte Receptor Signaling), Natural Killer cell activation (NK signaling), etc. We also clustered the genes corresponding to different canonical pathways utilizing IPA methodology, out of these genes we identified the most significant genes with high FC-value.

3.3. Results

3.3.1 First-order kinetics: Path for complete tumour regression

Now we are recollecting the modeling of the spontaneous tumour regression process as per the methodology mentioned chapter 2. For the tumour and cellular parameters, we taken the same values as the adult case in the earlier chapter, having an initial tumour population of 2×10^7 malignant cells. We select the desired time of tumour extinction of 46 days, and from Figure 2.1 (b), we found that bias $M^* = 1.8986\times10^5$ cells (this is a relatively small amount with respect to the initial malignant cell population of 2×10^7 cells, i.e. Negative bias ≈ 1% of initial tumour load). Hence, using a simulation-step of 0.01 sec, we solved the separate set of the aforesaid equations (1) – (7) of chapter 2 to obtain the time-wise variation of the level of three antitumour entities (concentrations of DNA damage factor and of interleukin-2, and Cytotoxic T-cell population). We have used customized MATLAB codes for numerical simulation of the above tumour elimination process already discussed in chapter 2. The tumour population trajectory definitively meets the time-axis at 46 days and the tumour cell population becomes zero from that time onwards.

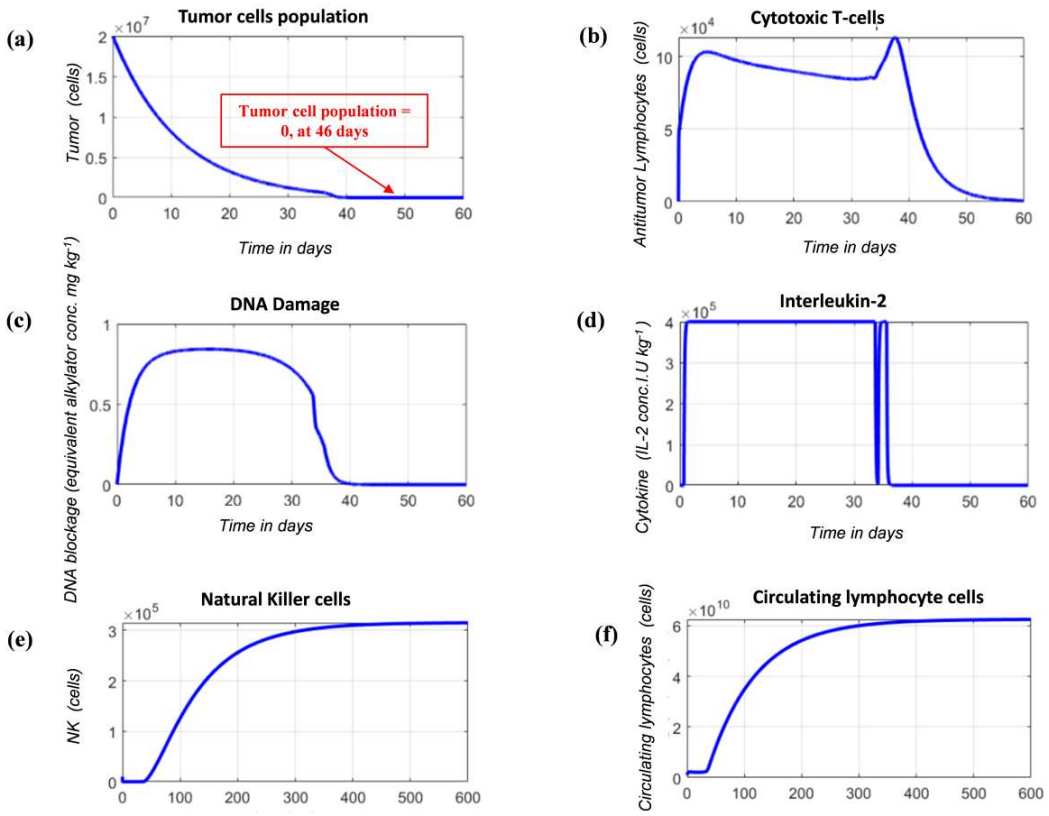

Figure 3.1 Permanent elimination of malignant melanoma tumour under first-order kinetics

(a) Tumour cell population shows consistent decline with time, with complete elimination of the malignant tumour at 46 days by following first order kinetics with a small negative biasing.

(b) Time-wise bimodal profile of cytotoxic T-cell needed for eliminating tumour cells. **(c)** Time-wise unimodal profile of DNA damage level needed for extinction of tumour cells (damage of DNA is estimated in terms of the equivalent amount of alkylator substance (as dacarbazine) which produces a similar amount of DNA damage, please see text).

(d) Time-wise stationary concentration profile of Interleukin-2 needed for tumour extinction (the curve maintains a uniform level).

(e) Time-wise saturation concentration profile of Natural Killer cells needed for tumour extinction (the curve maintains a saturated level).

(f) Time-wise saturation concentration profile of Circulating lymphocyte cells needed for tumour extinction (the curve maintains a saturated level).

3.3.2 Overall profile of Permanent Tumour Remission process

Let us now recapitulate the characteristic of complete tumour regression process from section 2.3.2.5 of chapter 2. There by performing multiple simulations, we noted that there is a general common pattern, which indicates that to induce complete tumour regression, the three antitumour entities should have three distinct temporal profiles:

(a) *Monophasic intensity* for the activation of DNA damage (e.g. chemical alkylation), showing one peak temporally (Figure 3.2a).

(b) *Biphasic intensity* for lymphocyte activation, displaying two temporal peaks (Figure 3.2b)

(c) *Uniform intensity* for interleukin-2 activation, where constancy in level is observed (Figure 3.2c).

(d) *Saturation intensity* for Natural killer cells and Circulating lymphocytes activation, showing saturated curve (Figure 3.2d)

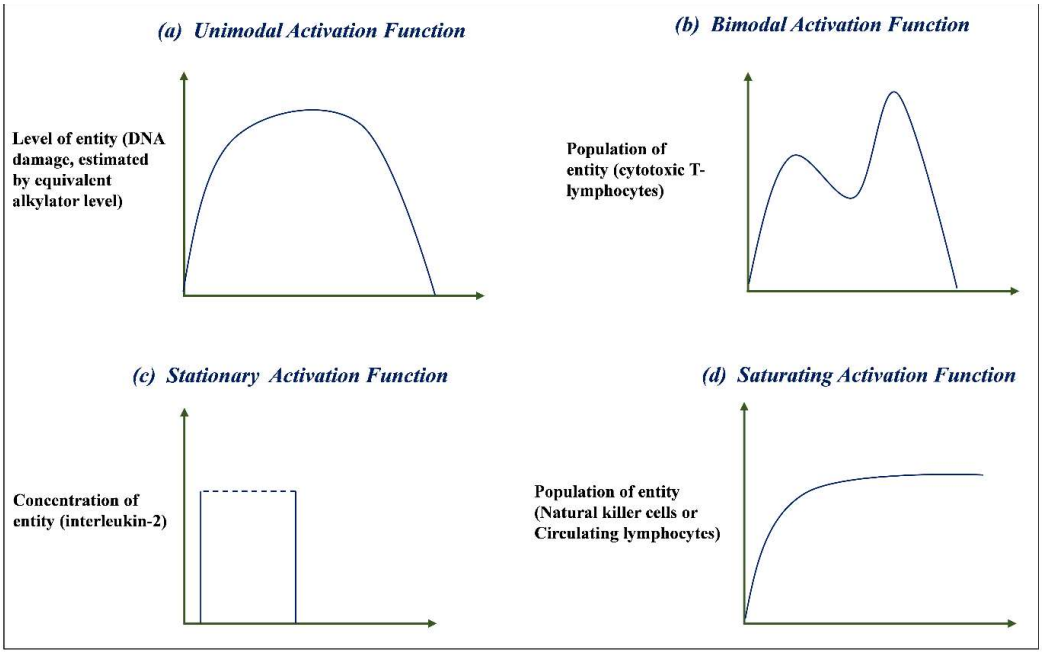

Figure 3.2 To enable permanent regression of malignant tumour with different initial conditions, the antitumour-entities are found to have the following common time-wise varying patterns: **(a)** Unimodal temporal intensity of DNA blockade factor, **(b)** Bimodal temporal intensity of Cytotoxic T-cell, **(c)** Uniform stationary temporal intensity of Interleukin-2, **(d)** Saturating temporal intensity of Natural killer cells and Circulating lymphocytes.

3.3.3 Experimental validation

We now furnish experimental findings of complete permanent tumour regression that provide substantiation and corroboration to our mathematical theoretical model of complete elimination of tumour by *the five-pattern temporal profile* (**Figure 3.*2***), namely the activation of antitumour lymphocyte (bi-modality), DNA damage or impairment (unimodality), interleukin-2 (stationarity), circulating lymphocyte (saturation) and NK cell (saturation).

3.3.4. Malignant melanoma elimination

3.3.4.1. Melanoma microarray data preprocessing

The microarray raw data file of the spontaneous regression of malignant melanoma tumour was downloaded from the ArrayExpress system (E-MEXP-1152) and analyzed using the Bioconductor package on the R platform. Furthermore, one-way ANOVA was performed for five different time points (taking time t_0 as the reference) to find the differentially expressed genes (DEGs) based on *p* value and FC value (p value < 0.05 and FC > 2). Finally, we got total 70 DEGs at time point t_1, 322 DEGs at time point t_2, 1147 DEGs at time point t_3, and 1349 DEGs at time point t_4 (DEGs-related information are provided in Appendix-III (A); in the Tables there, the lists of the successive genes were truncated at 100). The ANOVA analysis results showing the differentially expressed genes (DEGs) is displayed in Figure **3.3**.

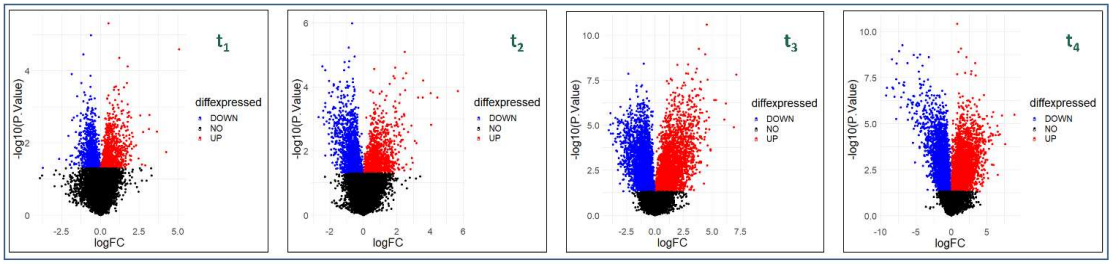

Figure 3.3 Volcano plots for differentially expressed genes. ANOVA analysis results showing DEGs plot: blue color signifies the downregulated genes, red color signifies the upregulated genes, and black color signifies the non-significant genes.

3.3.4.2. Identification of signaling pathways

Permanent endogenous melanoma regression microarray data of pigs were investigated by IPA. We assessed the antitumour T-cell activation intensity by the level of the IPA's T-cell pathway, named "PD-1/PD-L1 cancer immunotherapy pathway". Similarly, we gauged the DNA impairment level by the IPA pathway "G2/M DNA Damage Checkpoint Regulation". Likewise, we estimated the Natural-Killer cell level by IPA pathways "NK

cell signaling". Furthermore, we assay the Circulating lymphocyte level by the IPA pathway ("Leucocyte extravasation signaling"); indeed, one knows that during immune response, the extravasation of circulating leucocyte through the vascular wall into tumourous tissue, correlates with activation of circulating lymphocytes [83].

Thus, we found the specific temporal behaviour of the activation levels of cytotoxic T-lymphocytes (Figure 3.4 (a)), DNA impairment (Figure 3.4 (b)), circulating leucocytes (Figure 3.4 (c)), and natural killer cells (Figure 3.4 (d)). It is evident that the first and second curves (Figure 3.4 (a, b) follow respectively the bimodality and unimodality pattern of Figure 3.1 (a, b). Also, the third and fourth curves (Figure 3.4 (c, d)) both follow the saturation pattern of Figure 3.1(f, e). Thus the four experimental curves of Figure 3.4 closely correspond to the mathematically predicted patterns of Figure 3.1.

To show that our theoretically calculated model of tumour regression (Figure 3.1) adequately describes the experimentally observed tumour regression behaviour (Figure 3.4), we used the goodness-of-fit criterion (Kolmogorov-Smirnov test). Accordingly, we found that the experimental graphs of panels (a)–(d) of Figure 3.4 are satisfactorily accounted respectively by the corresponding theoretical graphs of panels (a, b, f, e) of Figure 3.1, and the corresponding goodness-of-fit Kolmogorov-Smirnov's statistical test was satisfied ($\alpha = 5\%$).

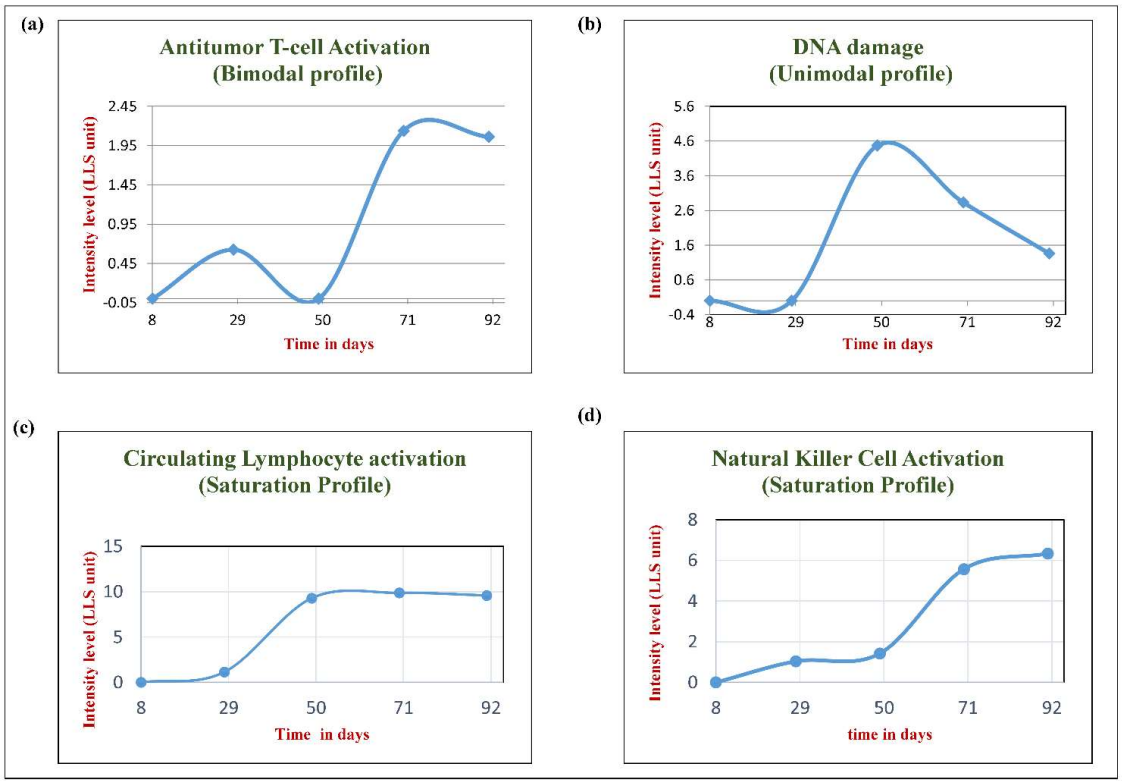

Figure 3.4 Comprehensive experimental validation of the prediction of the computational model. Behaviour of the various formulated entities needed for malignant tumour regression (melanoma) are shown, the entities being antitumour T-cells, DNA damage, Circulating lymphocytes, and Natural killer cells. (a)–(d) Activation of the biological readouts obtained using microarray data of the respective tissues at the various time-points, the vertical *y*-axis is in LLS units, i.e., log level of significance (i.e., *–log* (*p*-value)). Regarding the four curves, it is evident that their activations are respectively of bimodal (panel (a)), unimodal (panel (b)), and saturation patterns (panel (c), (d)), which are also predicted by our computational model developed theoretically for tumour regression (patterns of the computationally predicted theoretical curves are in Figures 3.1).

Now, we arrive at the molecular biological basis of aforesaid biological entities involved in permanent endogenous tumour regression. Using genetic analysis, we also found the genes associated with these different entities, which we elucidate below. Table 3.1 (left three columns) summarizes the main aspects of our findings.

3.3.4.3. Identification of genes

We found the signaling pathways and related genes for spontaneous regression using IPA. We selected the gene based on FC-value from the cluster of gene obtained from IPA, for different biological classes. Accordingly, we have furnished below the two lead exemplar genes for the antitumour functions as follows (also see Table 3.1, right two columns):

(a) DNA Damage-related genes: *CDC2, CHEK*;

(b) Interleukin-2 signaling-related genes: *IL2RG, AKT3*;

(c) Natural-killer cell signaling-related genes: *NKG2D, KLRK*;

(d) Cytotoxic T-cell activation-related genes: *TRGV5, CD28*;

(e) Circulating lymphocyte activation-related genes: *TCA, CCL5*.

Table 3.1 Biologically-based experimental corroboration of the computed activation functions of the antitumour entities which enable complete tumour elimination: The characteristic computed functions [Eqs (1)–(4), (6) of chapter 2] are in the first column, rows 2–6), and for each of these functions, their corresponding biological significance and relationships are provided in the other columns. The negative bias function is also included as row 7)

Characteristic function predicted by mathematical model	Biological entities involved	Biological basis of the characteristic function	Exemplars of genes involved in the antitumour characteristic	Illustrative findings
Monophasic Activation (DNA blockage)	DNA. Chemomodulation: Cell multiplication blockage.	Build-up and then decay of DNA chemomodulative or blockage activity.	Cell kinase gene: *CDC2, CHEK1* Cell cycle gene: *CCNB1, CCNB3*	Figure 3.1(c), Figure 3.4(b)
Biphasic activation (Cytotoxic T-cell)	Lymphocyte enhancement: Lysis of tumour cells.	Second rise (biphasicity) in T-cell population due to decline of chemomodulation, i.e., decrease in blockage of T-cell growth.	T-cell receptor activation: *TRGV5* gene, CD28 gene. G-protein coupled receptor activation: *CALCR* gene, CBLB gene.	Figure 3.1(b), Figure 3.4(a)
Uniform Stationary activation (Interleukin-2)	Cytokine enhancement: Escalating the leucocyte-tumour cell interaction.	Toxicity limit of cytokine (homeostasis).	Interleukin-2 receptor gene: *IL2RG, AKT3* gene. Transmembrane protein: *CD74, GRB2* gene.	Figure 3.1(d), Figure 3.5(a)
Saturating Activation (Natural killer cell)	Natural killer cell function (normal tissue protection).	Equilibrium state after Tumour regression.	NK cell activator gene: *NKG2D* gene, *STAT4* gene Actuates NK cell function activators: *KLRK1* gene, *MAP3K12* gene.	Figure 3.1(f), Figure 3.4(d)
Saturating Activation	Circulating lymphocyte	Equilibrium state after	Chemokine ligand 1	Figure 3.1(e),

(Circulating lymphocyte)	function (host defense).	Tumour regression.	activity: *TCA* gene - Actuates lymphocytes & monocytes. Rantes ligand activity: *CCL5* and *PRKCB* genes - Actuates lymphocyte & monocytes.	Figure 3.4(c)
Negative biasing	Apoptosis pathway	Elimination of residual tumour cells.	Extrinsic apoptosis pathway activator genes: *CASP7* gene, *GZMB* gene. Intrinsic apoptosis pathway activator gene: *BCL2L1* gene	Figure 2.1(b),

3.3.5 Negative bias related genes: CASP7, GZMB

Now, for identifying the genes that function as effecting the negative bias in tumour cell reduction trajectory, we have selected the genes which are responsible for the apoptosis process of the tumour cells, namely the Perforin/Granzyme apoptosis pathway activator genes: *CASP7, GZMB*. In other words, the pathway is a serine protease pathway, which is a primary signaling route used by cytotoxic T cells and natural killer cells to eliminate virus-infected or mutated malignant cells [84]. Cytotoxic T cells have perforin, which is a pore forming complex, while Granzyme B (GZMB) is an apoptotic signaling molecule that is able to initiate apoptotic signal by the process of exocytosis. After getting into the mutated malignant cell, this GZMB molecules interact with BID protein of the cells, which is actually the BH3 interacting domain death family protein that initiates the apoptosis process by activating caspase 7. As shown in Table 3.2, the expression values of these two

genes (*CASP7* and *GZMB*) increased from time point t_1 through t_4, while the tumour regression process advanced with time and this regression process was maximum at t_4 time point (where the tumour has completely regressed and become extinct). Indeed, the aforesaid proteins actuated by these two genes were able to attack and lyzed all the residual tumour cells in the last time segment (t_3- t_4), thereby preventing tumour relapse.

Table 3.2 Genes inducing Negative bias with their activity values at different time points.

Gene Name	Log_2FC value (at time t_1)	Log_2FC value (at time t_2)	Log_2FC value (at time t_3)	Log_2FC value (at time t_4)	*p.* value	*F*	Average Expression
GZMB *(Granzyme-B)*	-0.07314	0.525236	1.124219	2.326586	0.00011	10.0495	6.086244
CASP7 *(Caspase-7)*	-0.02369	0.12626	0.570303	1.488125	0.03849	4.8372	7.215214

3.3.6 Malignant histiocytoma elimination

Here complete endogenous regression of malignant histiocyte tumour in rodent system was analyzed. The experimental investigation is available, along with biochemical parameters [85]. In Figure 3.5 we delineated the temporal behaviour of the relevant parameters, which we have calculated from that initial study. The experimental study was done for 32 days, and two types of tumour regression regimes were observed: (i) Early regressor animals, where tumour size increased up to the 10^{th} day, then tumour regression occured, (ii) Late regressor animals, who display tumour size increased till about the 20^{th} day, and tumour regression started thereafter [85]. Hence, to observe the tumour decline process for a substantial duration, we analyzed the findings of the first group, where regression deviation was observed longer, namely across 22 days (in the second group, the

regression duration was much shorter, only for 12 days). We note that the experimental graphs showing temporal profile of interleukin-2 and DNA impairment (Figures 3.5(a, b)) are satisfactorily described by the corresponding theoretical graphs predicted (Figure 3.1(d, c)), the Kolmogorov-Smirnov statistical test of goodness-of-fit being also satisfied (α = 5%).

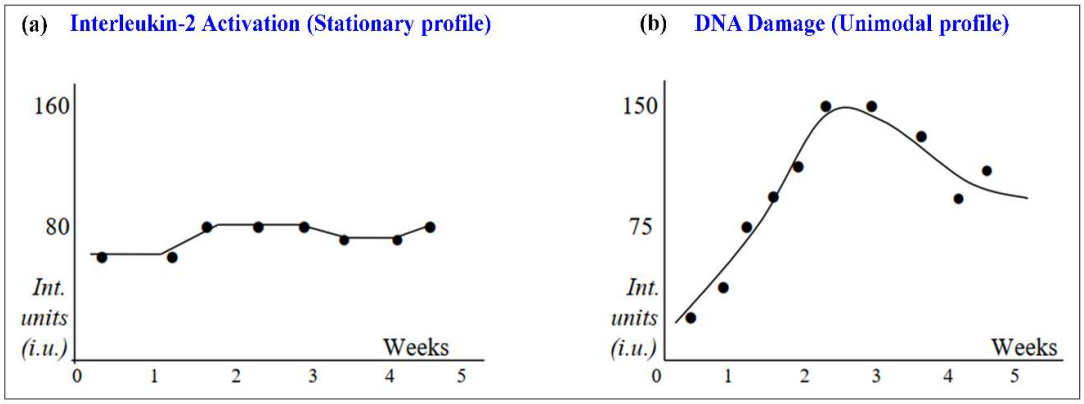

Figure 3.5 Permanent regression of malignant tumour: Empirical confirmation of the activation functions of the computational model, the tumour being malignant histiocytoma. (a) Interleukin-2 level as tumour regression ensues across time: the activation level is practically stationary. (b) Intensity of DNA damage, as gauged by level of TNF-α that induces DNA strand breaks. Note that here the activation function is unimodal.

3.4. Discussion

The episodic natural phenomenon of spontaneous regression of malignant tumours occurs in many types of cancer, where the tumour is completely eliminated without any toxicity effects on the animal or patient. Making intensive endeavors to understand this unique natural phenomenon can provide much insight into the possibility of replicating such a regression process on a clinical tumour without appreciable side-effects. One of the main concerns of oncological treatment is the toxic side effects of anticancer agents, which often limit the therapeutic intervention, leading to the deterioration of the patient. The non-toxic nature of spontaneous tumour regression is an added inducement to researchers on why the process

should be investigated well.

In our present study, we have developed an integrative mathematical systems biology-based approach to the permanent spontaneous tumour regression process. We have shown that this tumour regression and extinction process is mainly due to first-order kinetics producing tumour cell decline, with a small negative bias necessary for the extinction of the residual tumour cells. We have also provided biological validation of our theoretical mathematical approach utilizing experimental findings of the malignant melanoma regression, as a case-study model paradigm. Furthermore, our approach shows how three complementary entities (DNA blockage, antitumour lymphocyte, and cytokine activation) are orchestrated synergistically at different time segments to produce complete extinction of tumour cells.

Figure 3.1 (b, c, d) panels show how the inputs of cytotoxic T-lymphocytes, DNA blockage, and interleukin-2 need to change time-wise for the melanoma tumour to undergo complete eradication, whether by the endogenous way (spontaneous regression) or by the exogenous way (therapy-induced regression). In the spontaneous regression mode, these inputs are themselves generated by the host tissue. The vertical axes of the three panels furnish the time-wise input produced by the host tissue. For instance, the DNA blockage axis (vertical axis in Figure 3.1c) shows the amount of DNA blockage expressed equivalently in terms of DNA alkylation level, measured in terms of equivalent dacarbazine units. Regarding therapy-induced regression, these three inputs (T-lymphocytes, chemotherapy drug, and interleukin-2) will be administered externally at the time-wise injection rate given in the vertical axes of the three panels. For instance, the DNA blockage axis shows the dacarbazine dose (in mg/day/kg body weight of the subject) required for melanoma tumour extinction.

3.4.1 Practical implementation: Enforcement of tumour extinction–computational feedback approach

Our model applied for both endogenous and exogenous tumour regression, the latter implying tumour regression under therapy. Hence our formulation has incisive implications for clinical treatment. A seminal aspect of our formulation is the incorporation of feedback approach (Figure 2.5), whereby the antitumour entities (DNA damaging entity, interleukin-2, and lymphocytes) are primally and accurately varied with time, such that the tumour cell population undergoes extinction in the specific time duration (around 40–60 days), by following an optimum natural exponentially decreasing trajectory (with negative bias, Figure 2.1(b)). In other words, this declining curve furnishes the guidance for a trajectory which needs to be followed by the tumour cell population to reach a population of zero in the definitive time period. During the simulation process, after suitable time interval (time-step), one updates the tumour cell population which has declined a bit in the earlier time interval due to the action of the antitumour entities (Figure 2.6). This updated tumour cell population is used (at the next time-step) to determine the new values of antitumour entities, which are implemented iteratively in the simulation loop, and the tumour cell population declines a further bit, so that across successive time intervals, the tumour cell population follows the exponentially decreasing curve to extinction.

As time progresses, and if at any point, there is any incongruence of the actual tumour cell population from the mathematical tumour cell population of the exponential curve, the feedback control system (Figure 2.6) acts by altering the values of the antitumour entities, so that the error is corrected, and the trajectory of the tumour cell population is also corrected, thereby following the exponential curve. The feedback control approach is in

marked contrast to the customary approach in clinical oncology, where the antitumour entities are given in fixed-dose planned out beforehand, and the dosages do not adapt to the variable patient response, and neither to the varying tumour load day-to-day. There were earlier attempts to use feedback control system for antitumour therapy [86] but, as far as we know, they have not been on the lines proposed here, namely trajectory guidance control that enforces the tumour system to persistently reach the target (zero malignant cell population), with inbuilt ability for error correction and adaptation.

3.4.2 Clinical translation: Towards complete tumour elimination by negative biasing

We can now clarify the modus operandi for clinical applications. We may formulate the generalization of the tissue-induced process of endogenous tumour elimination, so as to develop the therapy-induced process of exogenous tumour regression. For permanently eliminating the tumour, Eqs (9), (11), and (12) of chapter 2 respectively provides the required time-varying profile of the intensities of the three entities in the tissue: (i) DNA damage, $D(t)^{\ddagger}$, (ii) cytotoxic lymphocyte population $A(t)^{\ddagger}$, and (iii) cytokine interleukin-2 concentration, $C(t)^{\ddagger}$. Likewise, for clinical applicability on patients, we need to induce the exogenous tumour elimination by externally administering therapeutic agents that would produce the requisite temporally-altering levels of the aforesaid entities (i)–(iii), namely the three agents would be a chemotherapeutic agent (e.g., dacarbazine, or cyclophosphamide etc.), cytotoxic T-cells, and interleukin-2 preparation (Figure 2.2). Each of these agents can be given by time-varying continuous intravenous infusion by an injected fluctuating dose-rate function, $v_{\mathrm{D}}(t)^{\ddagger}$, $v_{\mathrm{A}}(t)^{\ddagger}$ and $v_{\mathrm{C}}(t)^{\ddagger}$ (Section 2.2.7), which can be readily calculated from the required levels of the three entities in the tissue $D(t)^{\ddagger}$, $A(t)^{\ddagger}$ and $C(t)^{\ddagger}$ (Figure 2.6 and Section 2.2.7). Thus, if those temporal dose-rate patterns of the three therapeutic agents are injected, then the levels of those agents in the tissue would be $D(t)^{\ddagger}$,

$A(t)^{\ddagger}$ and $C(t)^{\ddagger}$, whereby the tumour cell population would follow the trajectory in Figure 3.6, becoming extinct at time t_p days, with no tumour recurrence nor toxicity to the patient.

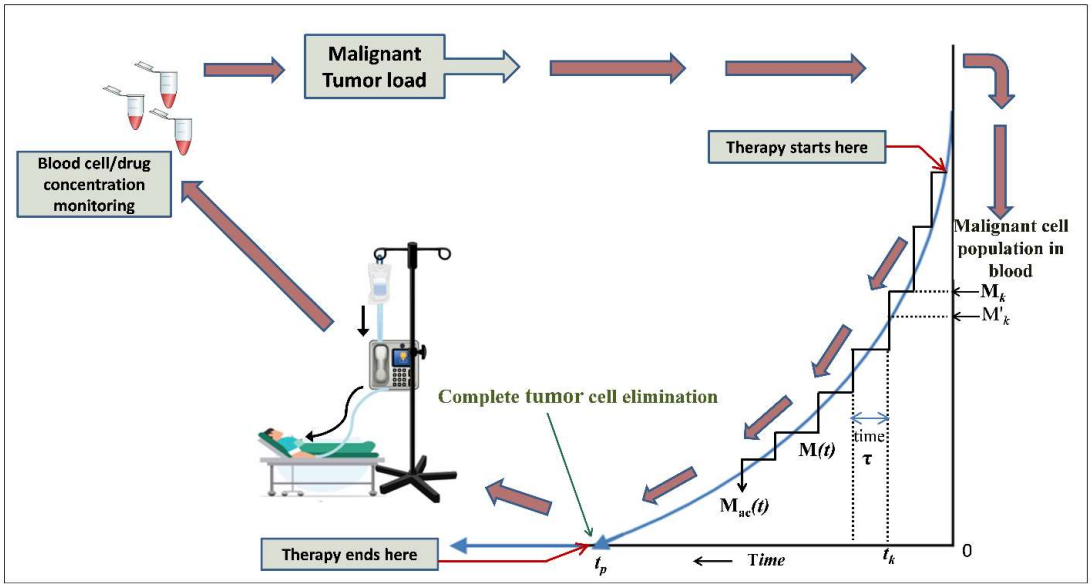

Figure 3.6 Clinical implementation of the feedback-based tumour elimination procedure, using cytologically-based tumour burden monitoring procedure (e.g., liquid biopsy in blood, or Spect imaging) at weekly time intervals.

3.5. Conclusions

Using a systems biology methodology, we have endeavored to analyse the mechanisms behind spontaneous cancer regression, and how normal tissue is protected during this tumour cell elimination. We also elucidated the treatment implications, so that the mechanistic knowledge could be utilized for therapeutically replicating the tumour regression process and normal tissue protection on clinical patients. Our approach was corroborated by experimental findings from pig and rodent studies. Indeed, a significant finding of our investigation is that this first order kinetics-based tumour regression is enabled by three cytotoxic entities: DNA blockage, interleukin-2 and antitumour T-lymphocyte activation. We found the microarray analysis of regressing tumours shows that

the time-wise profile of these three entities mathematically follows the following temporal patterns respectively, (i) unimodal inverted V-function, (ii) Bimodal M- function, and (iii) stationary-step function. These entities offer a tri-phasic cytotoxic profile that has been timed-orchestrated for eradication of all malignant cells We have also identified the gene expression levels related to above mentioned cytotoxic entities: (i) DNA-damage G2/M checkpoint regulation (CDC2 and CHEK genes); (ii) Interleukin-2/15 chemokine signalling (IL2RG and IKT3 genes); and (iii) T-lymphocyte signalling (TRGV5 and CD28 genes). The ability to eradicate the residual tumour correlates with our observation that the genes CASP7 and GZMB are indicators of Negative bias dynamics. In this chapter we have provided the dose-time profiles of aforesaid antitumour entities using the negative-biasing approach, so that melanoma tumour may undergo permanent extinction by mimicking the spontaneous tumour regression dynamics.